Quantum Oscillations in Two-Dimensional Insulators Induced by Graphite Gates

Jiacheng Zhu,[1] Tingxin Li,[1] Andrea F. Young,[2] Jie Shan,[1,3,4] and Kin Fai Mak[1,3,4,*]
[1]School of Applied and Engineering Physics, Cornell University, Ithaca, New York 14853, USA
[2]Department of Physics, University of California, Santa Barbara, California 93106, USA
[3]Laboratory of Atomic and Solid State Physics, Cornell University, Ithaca, New York 14853, USA
[4]Kavli Institute at Cornell for Nanoscale Science, Ithaca, New York 14853, USA

(Received 2 August 2021; accepted 4 November 2021; published 10 December 2021)

We demonstrate a mechanism for magnetoresistance oscillations in insulating states of two-dimensional (2D) materials arising from the interaction of the 2D layer and proximal graphite gates. We study a series of devices based on different 2D systems, including mono- and bilayer T_d-WTe_2, $MoTe_2/WSe_2$ moiré heterobilayers, and Bernal-stacked bilayer graphene, which all share a similar graphite-gated geometry. We find that the 2D systems, when tuned near an insulating state, generically exhibit magnetoresistance oscillations corresponding to a high-density Fermi surface, in contravention of naïve band theory. Simultaneous measurement of the resistivity of the graphite gates shows that the oscillations of the sample layer are precisely correlated with those of the graphite gates. Further supporting this connection, the oscillations are quenched when the graphite gate is replaced by a low-mobility metal, $TaSe_2$. The observed phenomenon arises from the oscillatory behavior of graphite density of states, which modulates the device capacitance and, as a consequence, the carrier density in the sample layer even when a constant electrochemical potential is maintained between the sample and the gate electrode. Oscillations are most pronounced near insulating states where the resistivity is strongly density dependent. Our study suggests a unified mechanism for quantum oscillations in graphite-gated 2D insulators based on electrostatic sample-gate coupling.

DOI: 10.1103/PhysRevLett.127.247702

The experimental observation of quantum oscillations in insulators has challenged the band theory of solids [1,2]. Proposals involving neutral fermions [3,4], excitons [5–7] and inverted bands [8–11] have been put forth to explain the puzzling observations. Recently, Wang *et al.* [12] reported magnetoresistance (MR) oscillations near the insulating state of monolayer WTe_2 encapsulated between thin hexagonal boron nitride (hBN) dielectrics (<10 nm) and graphite gates. They interpreted the results as evidence for charge-neutral fermions, engendering further theoretical proposals to explain the results [6,7,13]. However, the graphite gates play a crucial role for the observed MR oscillations; the replacement of the graphite gates by metallic gates causes a drastic degradation in the oscillations (extended data Fig. 10 in Ref. [12]). Moreover, some devices show two distinct oscillation frequencies with each frequency solely controlled by one of the two graphite gates (extended data Fig. 4 in Ref. [12]). These results call for closer scrutiny of the role of the graphite, which is itself a high-quality 2D electronic system.

In this Letter we demonstrate a capacitive mechanism by which MR oscillations in the sample are generated by oscillations in the graphite density of states (DOS). The basic idea is illustrated in Figs. 1(a) and 1(b). The sample and the graphite gate form the two plates of a capacitor. The total capacitance is determined by the geometrical capacitance and the quantum capacitances of the sample and the graphite gate. An external gate voltage maintains a constant electrochemical potential difference between the two plates. Because the graphite DOS oscillates under a perpendicular magnetic field (due to the formation of Landau levels), the total capacitance and therefore the carrier density in the sample oscillate accordingly; the sample and the gate are coupled [14,15]. Large MR oscillations near an insulating state of the sample, where the resistance is strongly dependent on the carrier density, are therefore expected. Here we demonstrate this ubiquitous phenomenon in various 2D materials, including mono- and bilayer WTe_2, $MoTe_2/WSe_2$ moiré heterobilayers and Bernal-stacked bilayer graphene. Coincident MR oscillations with identical gate voltage dependence for the oscillation frequency between the sample and the graphite gate are observed. The oscillations are quenched when the graphite gate is replaced by a $TaSe_2$ gate, a 2D metal with negligible DOS oscillations in moderate magnetic fields. Furthermore, a π phase shift in the MR oscillations between electron- and hole-doped bilayer graphene is observed. The results are fully consistent with the physical picture presented in Figs. 1(a) and 1(b).

The 2D sample of interest in all devices in this study is encapsulated between hBN dielectrics and top and bottom gates. The sample is contacted by appropriate metal

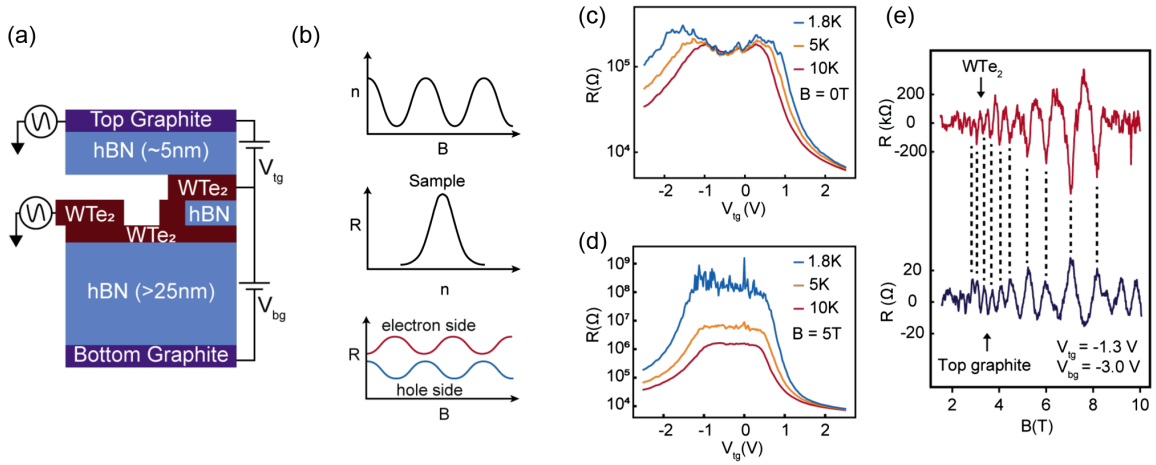

FIG. 1. (a) Schematic cross section for graphite-gated monolayer WTe_2 contacted by few-layer WTe_2 electrodes through a thin hBN barrier to avoid direct edge contact. (b) Schematic sample-gate capacitive coupling to induce MR oscillations. Top: carrier density oscillations in the sample versus magnetic field. Middle: density dependent resistance near an insulating state. Bottom: MR oscillations for electron doping and hole doping that show a π phase shift. (c),(d) V_{tg} dependence of the two-point resistance of monolayer WTe_2 at varying temperatures and $V_{bg} = 0$ V under $B = 0$ T (c) and $B = 5$ T (d). (e) Background-subtracted MR oscillations from slightly hole-doped monolayer WTe_2 and from the top graphite at $T = 1.8$ K. Dashed lines indicate the nearly perfect correlation of the two.

electrodes, which will be specified below, in order to minimize contact resistance. We focus on few-layer graphite with thickness 1–3 nm as the gate material and use $TaSe_2$ only in one occasion as a control experiment. The two gates allow independent tuning of the sample carrier density and the carrier density difference between the gates. In order to isolate effects from the top gate, we intentionally choose thinner hBN dielectric (~5 nm) for the top gate to increase its capacitive coupling to the sample and directly deposit the bottom gate onto SiO_2/Si substrates, which are known to degrade the electron mobility of the material [16]. These two strategies combined give negligible bottom gate-induced MR oscillations. Details of device fabrications are generic and have been reported elsewhere [16–18].

We first examine monolayer WTe_2 devices. Because the material is a quantum spin Hall insulator with helical edge states [19–21], the formation of electrical contacts to the bulk of monolayer WTe_2 requires the insertion of a thin hBN barrier in between the contact electrode and monolayer WTe_2. This is done in one of the contacts so that bulk conduction can be accessed [Fig. 1(a)]. We use few-layer semimetallic WTe_2 as the contact electrode to reduce contact resistance. We also insert few-layer graphite probes to contact the graphite top gate in order to simultaneously measure its resistance.

Figure 1(c) shows the top gate voltage (V_{tg}) dependence of the two-point resistance of monolayer WTe_2 at zero magnetic field and varying temperatures. The bottom gate voltage is fixed at $V_{bg} = 0$ V. A resistance plateau (~200 kΩ) nearly independent of temperature below 10 K is observed near $V_{tg} = 0$ V, where WTe_2 is close to the charge neutrality point. This is in contrast to the insulating behavior slightly away from charge neutrality, where the resistance increases (beyond 200 kΩ) with decreasing temperature (the insulatinglike behavior at high electron and hole doping is caused by the increase in contact resistance at low temperatures in a two-point measurement). The observation can be explained by the presence of lurking helical edge states that electrically short the insulating bulk of charge neutral WTe_2 [22]. The presence of lurking edge states in the sample is supported by the same plot as Fig. 1(c) under a perpendicular magnetic field $B = 5$ T [Fig. 1(d)]. The resistance no longer saturates at low temperatures; it displays the expected insulating behavior and reaches ~100 MΩ at 1.8 K. Because the external magnetic field breaks time reversal symmetry and induces significant back scattering in the helical edge states, lurking edge state conduction is no longer important and bulk conduction dominates.

Figure 1(e) shows the MR oscillations at 1.8 K for both the top graphite gate and slightly hole-doped WTe_2 at $V_{tg} = -1.3$ V and $V_{bg} = -3.0$ V, where WTe_2 displays insulating behavior. A smooth MR background is subtracted from the raw data to highlight the MR oscillations (Fig. S1 [23]). Unless otherwise specified, we will present the background-subtracted data at 1.8 K from now on. The observed MR oscillations in WTe_2 are consistent with the finding of Wang *et al.* [12]. The oscillations are almost perfectly correlated with those in the top graphite gate over a wide range of magnetic fields; the resistance dips in WTe_2 align with the resistance peaks in the graphite gate over multiple occurrences (marked by dashed lines).

To further illustrate the near perfect correlation, we examine the gate voltage dependence of the MR oscillations in Fig. 2. Figures 2(a) and 2(b) show in contour plots the V_{tg} dependence (at fixed $V_{bg} = 0$ V) of the MR

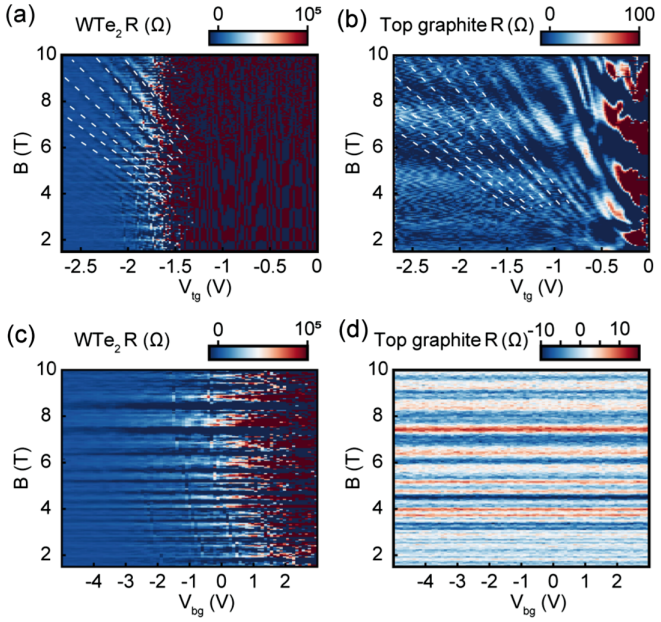

FIG. 2. V_{tg} (a),(b) and V_{bg} (c),(d) dependence of the MR oscillations from monolayer WTe_2 (a),(c) and from the top graphite gate (b),(d) at $T = 1.8$ K. (a),(b) Nearly identical Landau fans (white dashed lines) originating from $V_{tg} \approx 0$ V at $B = 0$ T are observed ($V_{bg} = 0$ V). (c),(d) The MR oscillations are independent of V_{bg} ($V_{tg} = -1.8$ V) and not intrinsic to WTe_2.

oscillations for slightly hole-doped WTe_2 and the top graphite gate, respectively. (See Fig. S2 in the Supplemental Material [23] for MR oscillations on the electron-doping side.) The graphite oscillations show a Landau fan with levels converging to near $V_{tg} \approx 0$ V at $B = 0$ T, as expected for typical quantum oscillations in graphite [24]. An almost identical Landau fan is also observed in WTe_2. (We cannot observe reliable MR oscillations for $V_{tg} > -1.5$ V because of the large resistance fluctuations near charge neutrality in WTe_2; the fluctuations are likely caused by the lurking edge states.) The nearly identical Landau fan structure of the two is further confirmed by fast Fourier transform (FFT) of the data in Figs. 2(a) and 2(b). (Fig. S3a and S3b in the Supplemental Material [23]). The oscillation frequency displays nearly identical V_{tg} dependence for the two cases.

We also examine the dependence of the MR oscillations on V_{bg} (at fixed $V_{tg} = -1.8$ V) in Figs. 2(c) and 2(d). The MR oscillations for both monolayer WTe_2 and the top graphite gate are independent of V_{bg} (also see the FFT data in Fig. S3c and S3d [23]). The absence of V_{bg} dependence in WTe_2 even though V_{bg} modulates its hole density shows that the MR oscillations are not intrinsic to WTe_2 but are induced by the top graphite gate. The bottom graphite gate induces no observable MR oscillation. The WTe_2 monolayer largely screens the electric field from the bottom gate to the top gate so that the MR oscillations of the top gate are independent of V_{bg}. The results are consistent with our intentional isolation of the top gate for inducing MR oscillations.

Next, we demonstrate the ubiquity of MR oscillations near the insulating states in several 2D materials induced by capacitively coupled graphite gates. We first examine bilayer WTe_2 contacted by semimetallic few-layer WTe_2. Whereas monolayer WTe_2 is a quantum spin Hall insulator, bilayer WTe_2 is a topologically trivial insulator without helical edge states [19,20]. The inset of Fig. 3(a) shows the doping dependent two-point resistance at zero magnetic fields. It shows a resistance peak exceeding 10 MΩ at charge neutrality, clearly demonstrating its insulating character. Near charge neutrality (the arrow in the inset), clear MR oscillations (without background subtraction) similar to those in monolayer WTe_2 are observed [Fig. 3(a)].

We also examined graphite-gated angle-aligned $MoTe_2/WSe_2$ heterobilayers, which form moiré superlattices because of the finite lattice mismatch between the two materials [25–27]. Pt contacts have been employed to reduce the contact resistance [25]. The physics of the system can be largely captured by a single-band Hubbard model [25,28,29]. The inset of Fig. 3(b) shows the doping dependent four-point resistance at zero magnetic field. Two

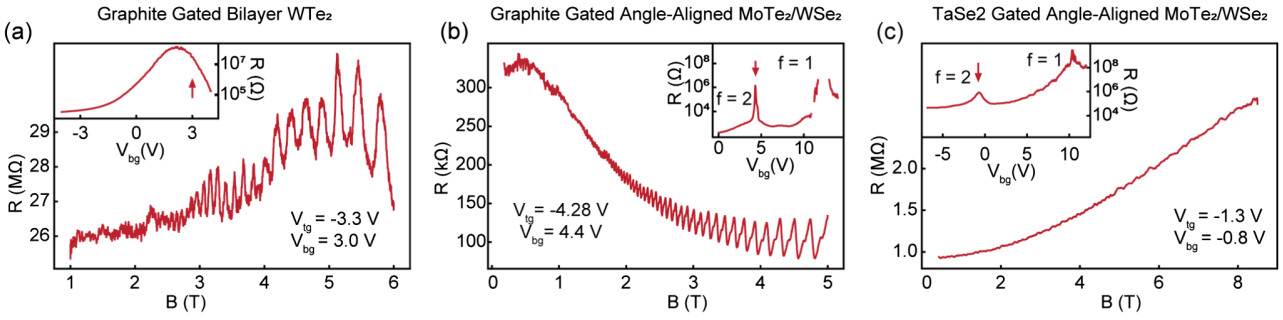

FIG. 3. (a)–(c) MR oscillations measured at $T = 1.8$ K for graphite-gated bilayer WTe_2 (a), graphite-gated (b), and $TaSe_2$-gated (c) $MoTe_2/WSe_2$ moiré heterobilayer. Inset of (a): Two-point resistance versus V_{bg} at $V_{tg} = -3.3$ V. Inset of (b): Four-point resistance versus V_{bg} at $V_{tg} = -4.28$ V. Inset of (c): Two-point resistance versus V_{bg} at $V_{tg} = -1.3$ V. The arrows mark where the MR oscillations are measured. The insulating states at filling factor 1 and 2 are labeled in (b),(c).

prominent resistance peaks at filling factor 1 and 2 are observed. They correspond to the Mott and the band insulating state, respectively [25]. A recent study has shown MR oscillations near the Mott insulating state [25]. In Fig. 3(b) we observe similar MR oscillations (without background subtraction) near the band insulating state (the arrow in the inset). To further illustrate the necessity of the graphite gate in inducing the MR oscillations, we replace the top graphite by a few-layer metallic $TaSe_2$ in a different device. Similar doping-dependent resistance compared to the graphite-gated device is seen in the inset of Fig. 3(c). However, no MR oscillations can be observed near the band insulating state [Fig. 3(c)]. Because of the much lower electron mobility compared to graphite, $TaSe_2$ shows negligible DOS oscillations under magnetic fields in this study [30] and therefore cannot induce MR oscillations in the sample. The result unambiguously confirms that the observed MR oscillations are induced by graphite.

The last example we will examine is Bernal-stacked bilayer graphene, which becomes a band insulator under a perpendicular electric field [31]. The high material quality allows us to quantitatively study the underlying mechanism responsible for the MR oscillations. Figure 4(a) shows a 2D map of the four-point resistance as a function of V_{tg} and V_{bg}. The arrows show the density and the electric field directions. The resistance maximum along the electric field direction corresponds to charge neutral bilayer graphene. The resistance at charge neutrality increases with electric field because of the opening of an energy gap [32]. The vertical feature near $V_{\mathrm{tg}} = 0$ V originates from a small region in the channel that does not overlap with the bottom gate. A representative density dependent resistance under a constant electric field ~0.2 V/nm is shown in Fig. 4(b). Clear MR oscillations (background subtracted) are observed in Fig. 4(c) for both electron- and hole-doping

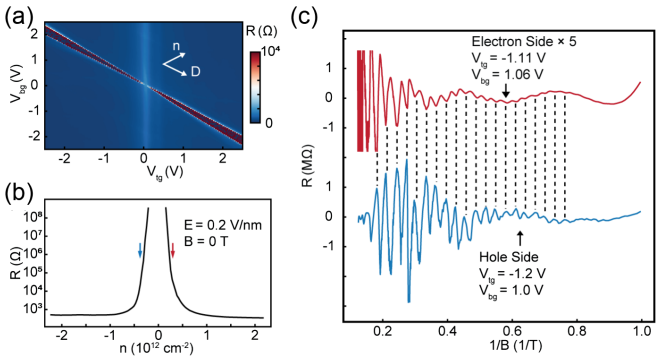

FIG. 4. (a) 2D map of the four-point resistance in bilayer graphene as a function of V_{tg} and V_{bg} at 1.8 K. The density and electric field axes are labeled. (b) Doping density dependent resistance under a constant electric field ~0.2 V/nm. (c) MR oscillations versus inverse magnetic field for electron- and hole-doped bilayer graphene marked by the arrows in (b). The vertical dashed lines mark the π phase shift.

[arrows in Fig. 4(b)]. Both the oscillation amplitude and frequency of the two cases are comparable because we have fine-tuned the gate voltages to maintain a constant carrier density in the top graphite gate. Interestingly, the oscillations are phase shifted by π between electron and hole doping; the dips for electron doping are aligned with the peaks for hole doping [vertical dashed lines in Fig. 4(c)].

The ubiquitous MR oscillations in different materials suggest an origin in the common graphite gated device architecture [Fig. 1(a)]. Our devices are typically asymmetric, with a bottom gate dielectric that is much thicker than the top gate dielectric. We therefore ignore the bottom gate for simplicity, and consider the capacitive coupling between the sample layer and the nearby top graphite gate. Crucially, in addition to the geometric capacitance, the quantum capacitance—arising from the finite electronic compressibility—of both the sample *and the graphite gate* must be accounted for. The total capacitance between the sample and graphite gate may be written as $C = (C_g^{-1} + C_{Qg}^{-1} + C_{Qs}^{-1})^{-1}$, where C_g is the geometric capacitance; C_{Qs} and C_{Qg} denote the sample and the graphite gate quantum capacitance, respectively. The carrier density under a constant electrochemical potential difference (V_{tg}) between the sample and the gate is $n = CV_{\mathrm{tg}}$.

The observed oscillations can be tied to the effect of the graphite compressibility and the graphite screening length on the charge carrier density of the sample layer. The low disorder and low effective mass of graphite mean that even at low magnetic fields, the graphite compressibility (or C_{Qg}) oscillates. In addition, the out-of-plane screening length of graphite (comparable to its thickness [33]) is modulated by the formation of Landau levels; this in turn induces oscillations in both the effective top gate dielectric thickness and therefore C_g. The two effects combined to generate net magneto-oscillations in C and thus the sample carrier density, which we denote Δn. Here a finite Δn can be induced even for insulating states because of the finite in-gap quantum capacitance of the sample ($C_{Qs} > 0$) arising from in-gap states responsible for hopping conduction at low temperatures. As a result, the sample resistance oscillates as $\Delta R \approx (dR/dn)\Delta n$, where (dR/dn) captures the density dependence of the resistivity. Notably, this effect is independent of oscillatory contributions to the sample quantum capacitance, C_{Qs}. It can be expected to apply to insulating regimes where sample carriers are localized and MR oscillations are not, otherwise expected.

This simple picture explains the ubiquitous MR oscillations in graphite-gated devices near the insulating states, where (dR/dn) is large. It also explains the quickly diminishing MR oscillations away from the insulating states (Fig. 2 and Fig. S4 of the Supplemental Material [23]), where (dR/dn) substantially drops in magnitude. In other words, the sample can only "sense" the oscillations in C_{Qg} when (dR/dn) is large, i.e., near an insulating state. The simple picture also explains the π phase shift in the MR

oscillations shown in Fig. 4(c), which arise due to the sign change in (dR/dn) from electron doping to hole doping [Δn remains nearly unchanged because we have kept a constant carrier density in the top graphite gate in Fig. 4(c)]. We further calibrate the magnetic-field-induced density oscillations in bilayer graphene in Fig. S5 [23].

We conclude by summarizing the necessary conditions for observing strong MR oscillations induced by the sample-gate capacitive coupling. First, because capacitors in series add *inversely*, the sample-gate separation needs to be small so that the effects of C_{Qg}^{-1} are amplified compared to C_g^{-1}. Second, the gate material needs to have high enough electron mobility, and low enough effective mass (i.e., large C_{Qg}^{-1}), to exhibit strong oscillations in C_{Qg}^{-1} under moderate magnetic fields (e.g., graphite). Finally, the sample needs to be near an insulating state where (dR/dn) is large in order to amplify the MR oscillations. Capacitively induced MR oscillations are expected when these conditions are met. However, we note that graphite gates may induce quantum oscillations in more subtle ways as well. For instance, compressibility oscillations in a proximal graphite gate may also modulate the screening of Coulomb repulsion in the 2D layer [34]. In small gap semiconductors, where Coulomb repulsion contributes significantly to the activation gap [35,36], this may lead to an additional effect capable of generating MR oscillations. In this picture, as the magnetic field is tuned, the compressibility oscillations induce oscillations in the activation gap, and consequently the resistivity of the proximal semiconductor. In addition, the oscillating electric field from sample-gate capacitive coupling in the device can also modulate the activation gap when it is electric field dependent; this can also create MR oscillations. In light of these potential mechanisms, caution is warranted in interpreting MR oscillations in insulating samples in terms of unproven mechanisms.

The authors acknowledge helpful discussions with Michael Zaletel and David Cobden. J. Z. acknowledges Kaifei Kang and Wenjin Zhao for discussions and experimental assistance. This work was supported by the U.S. National Science Foundation (Platform for the Accelerated Realization, Analysis, and Discovery of Interface Materials (PARADIM)) under Cooperative Agreement No. DMR-2039380 (device fabrication) and the ARO Grant No. W911NF-17-1-0605 (transport measurements). This work made use of the Cornell Center for Materials Research Shared Facilities which are supported through the NSF MRSEC program (DMR-1719875). A. F. Y. acknowledges the support of the Office of Naval Research Young Investigator program under Grant No. N00014-20-1-2609 and the EPIQS program of the Gordon and Betty Moore Foundation under Grant No. GBMF9471. K. F. M. acknowledges support from a David and Lucille Packard Fellowship.

*kinfai.mak@cornell.edu

[1] G. Li, Z. Xiang, F. Yu, T. Asaba, B. Lawson, P. Cai, C. Tinsman, A. Berkley, S. Wolgast, Y. S. Eo, D.-J. Kim, C. Kurdak, J. W. Allen, K. Sun, X. H. Chen, Y. Y. Wang, Z. Fisk, and L. Li, Science **346**, 1208 (2014).
[2] B. S. Tan, Y.-T. Hsu, B. Zeng, M. C. Hatnean, N. Harrison, Z. Zhu, M. Hartstein, M. Kiourlappou, A. Srivastava, M. D. Johannes, T. P. Murphy, J.-H. Park, L. Balicas, G. G. Lonzarich, G. Balakrishnan, and S. E. Sebastian, Science **349**, 287 (2015).
[3] D. Chowdhury, I. Sodemann, and T. Senthil, Nat. Commun. **9**, 1766 (2018).
[4] J. Knolle and N. R. Cooper, Phys. Rev. Lett. **118**, 096604 (2017).
[5] O. Erten, P.-Y. Chang, P. Coleman, and A. M. Tsvelik, Phys. Rev. Lett. **119**, 057603 (2017).
[6] P. A. Lee, Phys. Rev. B **103**, L041101 (2021).
[7] W. He and P. A. Lee, Phys. Rev. B **104**, L041110 (2021).
[8] J. Knolle and N. R. Cooper, Phys. Rev. Lett. **115**, 146401 (2015).
[9] J. Knolle and N. R. Cooper, Phys. Rev. Lett. **118**, 176801 (2017).
[10] H. Shen and L. Fu, Phys. Rev. Lett. **121**, 026403 (2018).
[11] Z. Han, T. Li, L. Zhang, G. Sullivan, and R.-R. Du, Phys. Rev. Lett. **123**, 126803 (2019).
[12] P. Wang, G. Yu, Y. Jia, M. Onyszczak, F. A. Cevallos, S. Lei, S. Klemenz, K. Watanabe, T. Taniguchi, R. J. Cava, L. M. Schoop, and S. Wu, Nature (London) **589**, 225 (2021).
[13] Y. H. Kwan, T. Devakul, S. L. Sondhi, and S. A. Parameswaran, Phys. Rev. B **104**, 125133 (2021).
[14] B. Skinner and B. I. Shklovskii, Phys. Rev. B **82**, 155111 (2010).
[15] T. Li, J. Zhu, Y. Tang, K. Watanabe, T. Taniguchi, V. Elser, J. Shan, and K. F. Mak, Nat. Nanotechnol. **16**, 1068 (2021).
[16] C. R. Dean, A. F. Young, I. Meric, C. Lee, L. Wang, S. Sorgenfrei, K. Watanabe, T. Taniguchi, P. Kim, K. L. Shepard, and J. Hone, Nat. Nanotechnol. **5**, 722 (2010).
[17] L. Wang, I. Meric, P. Y. Huang, Q. Gao, Y. Gao, H. Tran, T. Taniguchi, K. Watanabe, L. M. Campos, D. A. Muller, J. Guo, P. Kim, J. Hone, K. L. Shepard, and C. R. Dean, Science **342**, 614 (2013).
[18] Y. Tang, L. Li, T. Li, Y. Xu, S. Liu, K. Barmak, K. Watanabe, T. Taniguchi, A. H. MacDonald, J. Shan, and K. F. Mak, Nature (London) **579**, 353 (2020).
[19] Z. Fei, T. Palomaki, S. Wu, W. Zhao, X. Cai, B. Sun, P. Nguyen, J. Finney, X. Xu, and D. H. Cobden, Nat. Phys. **13**, 677 (2017).
[20] S. Wu, V. Fatemi, Q. D. Gibson, K. Watanabe, T. Taniguchi, R. J. Cava, and P. Jarillo-Herrero, Science **359**, 76 (2018).
[21] X. Qian, J. Liu, L. Fu, and J. Li, Science **346**, 1344 (2014).
[22] Y. Shi, J. Kahn, B. Niu, Z. Fei, B. Sun, X. Cai, B. A. Francisco, D. Wu, Z.-X. Shen, X. Xu, D. H. Cobden, and Y.-T. Cui, Sci. Adv. **5**, eaat8799 (2019).
[23] See Supplemental Material at http://link.aps.org/supplemental/10.1103/PhysRevLett.127.247702 for details on methods, background subtraction, data on electron-doping side, FFT of oscillations and extracting density oscillations.
[24] J. Yin, S. Slizovskiy, Y. Cao, S. Hu, Y. Yang, I. Lobanova, B. A. Piot, S.-K. Son, S. Ozdemir, T. Taniguchi, K. Watanabe,

K. S. Novoselov, F. Guinea, A. K. Geim, V. Fal'ko, and A. Mishchenko, Nat. Phys. **15**, 437 (2019).
[25] T. Li, S. Jiang, L. Li, Y. Zhang, K. Kang, J. Zhu, K. Watanabe, T. Taniguchi, D. Chowdhury, L. Fu, J. Shan, and K. F. Mak, Nature (London) **597**, 350 (2021).
[26] E. C. Regan, D. Wang, C. Jin, M. I. Bakti Utama, B. Gao, X. Wei, S. Zhao, W. Zhao, Z. Zhang, K. Yumigeta, M. Blei, J. D. Carlström, K. Watanabe, T. Taniguchi, S. Tongay, M. Crommie, A. Zettl, and F. Wang, Nature (London) **579**, 359 (2020).
[27] X. Huang, T. Wang, S. Miao, C. Wang, Z. Li, Z. Lian, T. Taniguchi, K. Watanabe, S. Okamoto, D. Xiao, S.-F. Shi, and Y.-T. Cui, Nat. Phys. **17**, 715 (2021).
[28] F. Wu, T. Lovorn, E. Tutuc, and A. H. MacDonald, Phys. Rev. Lett. **121**, 026402 (2018).
[29] H. Pan, F. Wu, and S. Das Sarma, Phys. Rev. B **102**, 201104 (R) (2020).
[30] R. M. Fleming and R. V. Coleman, Phys. Rev. B **16**, 302 (1977).
[31] E. McCann and M. Koshino, Rep. Prog. Phys. **76**, 056503 (2013).
[32] Y. Zhang, T.-T. Tang, C. Girit, Z. Hao, M. C. Martin, A. Zettl, M. F. Crommie, Y. R. Shen, and F. Wang, Nature (London) **459**, 820 (2009).
[33] H. Miyazaki, S. Odaka, T. Sato, S. Tanaka, H. Goto, A. Kanda, K. Tsukagoshi, Y. Ootuka, and Y. Aoyagi, Appl. Phys. Express **1**, 034007 (2008).
[34] Y. Xu, C. Horn, J. Zhu, Y. Tang, L. Ma, L. Li, S. Liu, K. Watanabe, T. Taniguchi, J. C. Hone, J. Shan, and K. F. Mak, Nat. Mater. **20**, 645 (2021).
[35] M. S. Hybertsen and S. G. Louie, Phys. Rev. B **34**, 5390 (1986).
[36] D. Y. Qiu, F. H. da Jornada, and S. G. Louie, Phys. Rev. Lett. **111**, 216805 (2013).